

The role of solvent microstructure on the aging dynamics and rheology of aqueous suspensions of a soft colloidal clay

Chandeshwar Misra, Venketesh T Ranganathan, and Ranjini Bandyopadhyay*

Soft Condensed Matter Group, Raman Research Institute,

C. V. Raman Avenue, Sadashivanagar, Bangalore 560 080, INDIA

(Dated: December 22, 2024)

Abstract

The influence of solvent microstructure on the microscopic dynamics and rheology of aging colloidal smectite clay suspensions is investigated by performing dynamic light scattering and rheology experiments. Additives that can either induce or break-up the ordering of water molecules in an aqueous medium are incorporated in aqueous Laponite[®] clay suspensions. While the addition of sodium chloride, glucose and potassium chloride accelerates the aging dynamics of the Laponite particles in suspension and leads to rapid dynamical arrest, the presence of N,N-Dimethylformamide disrupts the aging and jamming dynamics of the particles. An increase in temperature leads to the breaking of hydrogen bonds in an aqueous suspension medium. Our experiments reveal an accelerated approach to dynamical arrest when the temperature of Laponite suspensions is raised. The aging dynamics and rheology of the samples are correlated with their microstructural details visualized using cryogenic electron microscopy. Our data demonstrate that the microscopic dynamics of aging Laponite suspensions show self-similar time-evolution, while their long-time aging behavior and nonlinear rheological responses are sensitive to the temperature of the suspension medium and the presence of additive molecules.

INTRODUCTION

The structure [1–5], dynamics [6–8] and flow properties [9–12] of suspensions of smectite clay minerals have been studied extensively in the literature. Sodium-montmorillonite, also referred to as sodium bentonite, and kaolinite are two examples of clay minerals belonging to the smectite group that are available in abundance in nature [13]. The phase and bulk behaviors of smectite clay minerals can be easily tuned by tuning inter-particle interactions. This has led to the widespread applications of these clay minerals as rheological modifiers and stabilizers in paints, wellbore drilling fluids, cosmetics, pharmaceuticals, agrochemicals, paper fillers, coating pigments and nanocomposites [14–19]. Aqueous suspensions of clays, eg. sodium-montmorillonite, have been widely used in studies to understand large scale geophysical phenomena such as river delta formation, landslides and earthquake-driven liquefaction. [20–22].

Hectorite clays, belonging to the smectite group, have layered structures [23]. A Hectorite clay mineral that is often used for studying physical aging and glass transition dynamics is the synthetic colloidal clay Laponite[®][24–26]. Laponite particles are monodisperse disks having diameters 25–30 nm and thickness ~ 1 nm. In powder form, Laponite particles exist as one-dimensional stacks called tactoids. When the particles are dispersed in an aqueous medium, water molecules diffuse into the intra-gallery spaces and hydrate the sodium counterions, thereby causing the tactoids to swell [27]. This results in the dissociation of Na^+ , which diffuse out of the stacks into the bulk aqueous medium due to osmotic pressure gradients. The dissociation of Na^+ , which gives rise to excess negative charges on the surfaces of Laponite platelets [28], increases with increase in clay concentration [26]. The edge of a Laponite particle consists of anhydrous oxides dominated by MgOH groups. In a medium of $\text{pH} < 11$, the particles acquire positive charges on their edges due to the dissociation of OH^- [29]. Owing to dissimilar charges on its edges and faces, Laponite particles can interact via face-to-face or edge-to-edge repulsions and edge-to-face attractive interactions [30, 31]. The screened electrical Debye layer (EDL) formed by the dissociation of Na^+ from Laponite platelets impose dynamical constraints on the particles in aqueous suspensions. The EDL evolves with time, and eventually, at a sufficiently long waiting time, t_w , the suspension gets arrested in a jammed state. In this state, each particle in the aqueous suspension is confined in a cage formed by its neighbors.

Although the aging dynamics and phase behaviors of Laponite suspensions have been broadly debated in the literature, almost all studies have focused predominantly on the dynamics of

Laponite particles in aqueous suspensions [2, 9, 24, 32–35]. Aqueous suspensions of Laponite with particle concentrations between 0.5% and 4.0% show a continuous buildup of structure in a physical aging process that arises due to a spontaneous and gradual evolution of the interparticle electrostatic interaction [1, 28]. The phase behavior, rheological properties and aging dynamics of aqueous Laponite suspensions, widely investigated in the literature, are very sensitive to the presence of additives such as acid and salt, suspension temperature, applied electric field and preparation protocol [26, 36–39]. It is reported that the sizes of cooperatively rearranging regions or dynamical heterogeneities in aging Laponite suspensions increase monotonically with increasing waiting time t_w and clay concentration [40].

In the present study, we focus our attention on the role of solvent microstructure on the aging dynamics and rheology of Laponite suspensions. We achieve control over the solvent microstructure by incorporating additives and by changing sample temperature, both of which alter the population and strength of hydrogen bonds in the suspension medium [41–43]. A hydrogen bond in water is formed due to the dipole-dipole attraction between the positively charged hydrogen atom of a water molecule and the negatively charged oxygen atom of a neighboring water molecule [43]. The hydrogen bonds that form between two water molecules arrange in tetrahedral configurations and are recognized as the most energetically favored structure of liquid water [44]. When NaCl, a kosmotrope (a molecule inducing structure formation in the aqueous medium [45–47]), is added to liquid water, Na^+ forms a contact pair with Cl^- and the dipolar water molecules form hydration shells around Na^+ [46]. The strong electrostatic ordering of water molecules leads to a reduction in their diffusion rates. Addition of the kosmotrope glucose to water disrupts the tetrahedrality of water structure and results in the formation of dense structured layers of water around the glucose molecule [48]. This reduces the number of free OH^- groups and increases the population of hydrogen bonds surrounding each glucose molecule in solution [49]. On the other hand, addition of a chaotrope (a molecule that disrupts the structure of the aqueous medium) such as N,N-Dimethylformamide (DMF) to liquid water disrupts inter-molecular hydrogen bonding, with the water molecules forming hydrogen bonds with the oxygen sites of DMF [45, 50, 51]. When KCl, another chaotrope, is added to liquid water, K^+ does not form a contact pair with Cl^- and a classic hydration shell is not produced [46, 47]. Even though Na^+ and K^+ are both alkali atoms, their distinct interactions with water arise from their different physical properties such as surface charge densities and relative sizes. It is reported that K^+ accelerates the breakdown of hydrogen bonding in water which results in faster diffusion of water molecules in the bulk [46]. Since the

disruption of hydrogen bonds by K^+ dominates over the strong coulombic interactions between the K^+ ions, KCl, despite being an inorganic salt, acts as a chaotrope. It is to be noted that Cl^- is a weak kosmotrope and accumulates water molecules around itself in aqueous solutions of NaCl and KCl.

We perform dynamic light scattering (DLS) experiments to study the effects of the local structure of the suspension medium on the microscopic dynamics of Laponite particles in aqueous suspensions. The DLS data is supported by rheological measurements of the viscoelastic moduli of aqueous Laponite suspensions in the presence of different additives and at several suspension temperatures. We observe that the addition of kosmotropes leads to an acceleration in the aging dynamics of aqueous Laponite suspensions. In contrast, the addition of DMF delays the transition of the samples to a dynamically arrested state. Surprisingly, in spite of its known chaotropic action [46], we observe that KCl accelerates the aging dynamics of Laponite suspensions. Finally, we perform cryogenic scanning electron microscopy (cryo-SEM) experiments to study the morphological changes in aqueous Laponite suspensions with and without additives. Accelerated aging dynamics, resembling the results obtained when kosmotropes are added to Laponite suspensions, are also observed when temperature of the suspension medium is raised. The microscopic aging dynamics are self-similar in the presence of all the additives and at all suspension temperatures explored here. Furthermore, the viscoelastic moduli, when scaled appropriately, superpose at low strains but are sensitive to both additives and temperature at long times and under large strains. Our results, which are interesting from the point of view of achieving control on the spontaneous aging dynamics and rheology of clay suspensions, are applicable to a wide range of minerals belonging to the group of Hectorite clays.

EXPERIMENTAL SECTION

Sample preparation

Laponite XLG[®] powder (BYK Additives Inc.) was dried in an oven at 120°C for more than 18 h to remove moisture. The dried powder was weighed and added to Milli-Q water (Millipore Corp., resistivity 18.2 M Ω -cm) which was continually agitated using a magnetic stirrer for 45 min. The additives NaCl (LABORT Fine Chem Pvt.Ltd.), glucose (Sigma-Aldrich), DMF (SDFCL Fine Chem Pvt.Ltd) and KCl (Sigma-Aldrich) were measured and added to de-ionized water prior to

the addition of Laponite powder. All the additives were used as received without any further purification.

Dynamic Light Scattering

DLS experiments were performed using a Brookhaven Instruments Corporation (BIC) BI-200SM spectrometer attached with a 150 mW solid-state laser (NdYVO₄, Coherent Inc., Spectra-Physics) having an emission wavelength of 532 nm. The details of the setup are given elsewhere [25, 26]. A glass cuvette filled with the sample was held in a refractive index matching bath filled with decaline. For the DLS experiments, a freshly prepared sample was filtered into the glass cuvette through a Millipore filter of diameter 0.45 μm using a syringe. The increase in the sample waiting time, t_w , was monitored continuously from the time at which filtration was stopped ($t_w = 0$ at the completion of the filtration procedure). The cuvette was sealed and quickly placed in the DLS instrument to record the decays of the intensity autocorrelation functions with increasing t_w . The temperature of the sample was controlled with a temperature controller (Polyscience Digital) equipped with a water circulation unit. A Brookhaven Instruments BI-9000AT digital autocorrelator was used to measure the intensity autocorrelation function of the scattered light: $g^{(2)}(q, t) = \frac{\langle I(q,0)I(q,t) \rangle}{\langle I(q,0) \rangle^2} = 1 + A|g^{(1)}(q, t)|^2$ [52]. Here q , $I(q, t)$, $g^{(1)}(q, t)$ and A are the scattering wave vector, the intensity at a delay time t , the normalized electric field autocorrelation function and the coherence factor, respectively. The scattering wave vector q is related to the scattering angle θ , $q = (4\pi n/\lambda) \sin(\theta/2)$, where n and λ are the refractive index of the medium and the wavelength of the laser, respectively. The decays of the normalized intensity autocorrelation functions, $C(t) = \frac{g^{(2)}(q,t)-1}{A}$, were measured for Laponite suspensions at different t_w . The normalized autocorrelation function for 12.2 mM (2.8% w/v) aqueous Laponite suspensions at several t_w are plotted vs. delay time t in Figure 1.

The normalized autocorrelation functions, $C(t)$ plotted in Figure 1, fit best to functions representing two-step decays for the entire range of waiting times explored. This indicates the presence of two relaxation time-scales corresponding to two distinct dynamical processes which can be fitted to the following equation [25, 26, 40]

$$C(t) = [a \exp\{-t/\tau_1\} + (1 - a) \exp\{-(t/\tau_{ww})^\beta\}]^2 \quad (1)$$

Fits to the above equation were used to extract τ_1 and τ_{ww} , identified as the time-scales associated

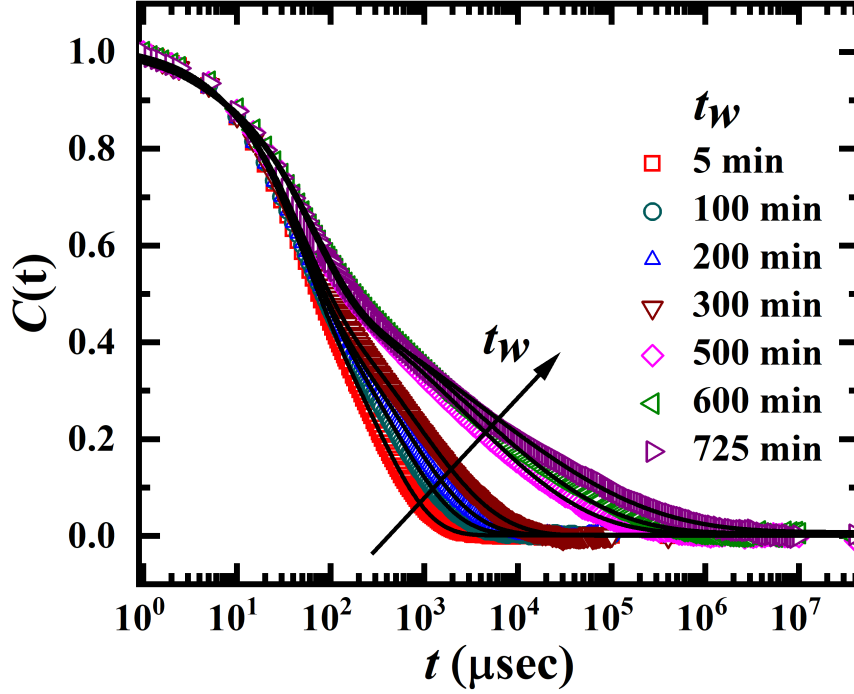


Figure 1: Normalized autocorrelation functions, $C(t)$, vs. delay time, t , at 25°C for 12.2 mM (2.8% w/v) aqueous Laponite suspensions. The solid lines are fits to eq 1.

with the β - and α - relaxation processes respectively. The faster β - relaxation involves the rattling motion of each particle inside its cage. The slower α - relaxation corresponds to the time-scale at which the particle can diffuse out of its cage in a process facilitated by cooperative rearrangements of the surrounding particles. The parameters a and $(1 - a)$ represent, respectively, the relative strengths of β - and α - relaxation processes, while β in eq 1 is a stretching exponent that quantifies the distribution of the α - relaxation times-cales. The average α - relaxation time can be defined as $\langle \tau_{ww} \rangle = (\frac{\tau_{ww}}{\beta})\Gamma(\frac{1}{\beta})$ [53], where Γ is the Euler Gamma function. The present work studies the approach of Laponite suspensions towards kinetic arrest by systematically monitoring the evolution of the average α - relaxation time, $\langle \tau_{ww} \rangle$, with increasing sample waiting time, t_w , in the presence of several additives and at different suspension temperatures. We have plotted τ_1 and $\langle \tau_{ww} \rangle$ vs. $1/q^2$ in Figure S1 for 12.2 mM aqueous Laponite suspensions without any additive (Figure S1a), in the presence of 260 mM DMF (Figure S1b) and 220 mM glucose (Figure S1c) at different waiting times, t_w . The fast and slow diffusion coefficients, D_1 and D_{ww} , for 12.2 mM aqueous Laponite suspensions in the presence of 220 mM glucose and 260 mM DMF were calculated according to

the protocol specified in Section 1(a) of the SI and are plotted in Figure S2 at a waiting time $t_w = 100$ min. It can be observed that both diffusion coefficients of aqueous Laponite suspensions decrease in the presence of glucose while they increase in the presence of DMF. This indicates accelerated and retarded aging dynamics of aqueous Laponite suspensions in the presence of glucose and DMF respectively.

Rheology

Rheological measurements were performed using a stress controlled Anton Paar MCR 501 rheometer. A double gap geometry (DG-26.7) with a gap of 1.886 mm, an effective length of 40 mm and requiring sample volume of 3.8 mL was used for dilute suspensions. For dense suspensions, a cone-plate geometry (CP-25) having cone radius $r_c = 12.491$ mm, cone angle 0.979° , measuring gap $d = 0.048$ mm and requiring sample volume of 0.07 mL was used. For the rheological measurements sample was loaded immediately after preparation. Loading memory effects were erased by shear melting the sample at a high shear rate of 1500 s^{-1} for 3 minutes to achieve a reproducible starting point for all experiments. The increase in the sample waiting time, t_w , was monitored continuously from the time shear melting was stopped. The temperature of the sample was controlled using a water circulation system (Viscotherm VT2). Silicon oil of viscosity 5cSt was used as a solvent trap oil to avoid solvent evaporation. The viscoelastic properties of aqueous Laponite suspensions in the presence of different additives and at different suspension temperatures were then investigated by performing oscillatory amplitude sweep experiments. By varying the strain amplitude (γ) from 0.1% to 500%, the storage modulus (G') and loss modulus (G'') were measured at a constant angular frequency (ω) of 6 rad/s. The time evolutions of storage modulus (G') and loss modulus (G'') of aqueous Laponite suspensions, aged to different t_w , were studied in the presence of the additives and at various suspension temperatures at a constant strain amplitude $\gamma = 0.1\%$ and angular frequency $\omega = 6$ rad/s.

Cryogenic Scanning Electron Microscopy (cryo-SEM)

Aqueous Laponite suspensions in the presence of kosmotropic and chaotropic molecules were visualized using a field-effect scanning electron microscope from Carl Zeiss with an electron beam strength of 5 kV. The samples were loaded in capillary tubes (Capillary Tube Supplies Ltd, UK)

with a bore size of 1 mm using capillary flow. The ends of the capillaries were sealed. Samples were kept undisturbed before imaging and were then vitrified using liquid nitrogen slush at temperature -190°C . The vitrified samples were cut and sublimated for 15 min at -90°C and then coated with a thin layer of platinum (thickness approximately 1 nm) in vacuum conditions using a cryo-transfer system (PP3000T from Quorum Technologies). The cryo-chamber temperature was kept at -190°C . Backscattered secondary electrons were used to produce surface images of the samples. ImageJ (Java 1.8.0_172, developed by Wayne Rasband, NIH, US) was used to analyze the cryo-SEM images.

RESULTS AND DISCUSSIONS

Effects of additives

Figure 2 shows the evolution of the slow α -relaxation time $\langle\tau_{ww}\rangle$ with waiting time, t_w , for a 12.2 mM (2.8% w/v) aqueous Laponite suspension (\diamond) with different concentrations of kosmotropic and chaotropic additives at a temperature 25°C . It is observed that when the concentrations of NaCl (shown in blue symbols) and glucose (shown in wine symbols) are increased, $\langle\tau_{ww}\rangle$ increases very rapidly as waiting time t_w is increased (Figures 2a and 2b). This can be understood by considering that the osmotic pressure gradients that arise due to formation of tight hydration shells around Na^+ and glucose molecules [54] can accelerate aging and lead to the observed rapid time-evolution of $\langle\tau_{ww}\rangle$.

It is seen from Figure 2c that when DMF (shown in dark yellow symbols) is added to Laponite suspensions, the divergence of $\langle\tau_{ww}\rangle$ is delayed when compared to the Laponite suspension without any additives (\diamond) at the same temperature. The addition of DMF molecules disrupts hydrogen bonds in water [45, 50, 51] and reduces the diffusion of the bulk water molecules into the intragallery spaces of the Laponite tactoids. This results in a significant reduction in the osmotic pressure gradients and a retardation in the aging dynamics. Surprisingly, when KCl (widely regarded as a chaotrope and shown in red symbols) is added to the medium, the aging dynamics of the suspensions are seen to accelerate (Figure 2d). We believe that enhanced inter-particle electrostatic screening, arising from the active participation of K^+ in the electric double layers (EDLs) formed by the Na^+ dissociated from Laponite particles, gives rise to the observed acceleration in the suspension aging behavior. An increase in the electrostatic screening between Laponite particles can

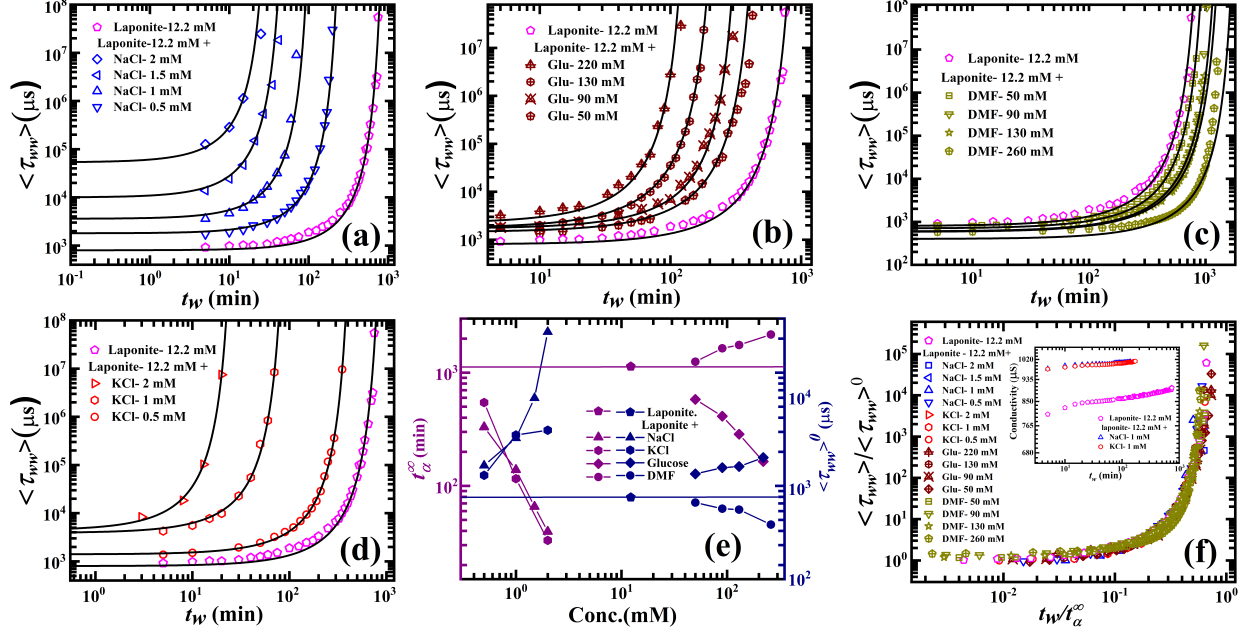


Figure 2: Mean slow relaxation time $\langle \tau_{ww} \rangle$ vs. waiting time t_w for 12.2 mM aqueous Laponite suspension without and with different concentrations of additives (a) NaCl, (b) glucose (Glu), (c) DMF and (d) KCl. The solid lines are fits to eq 2. (e) Horizontal and vertical shift factors, t_α^∞ (Vogel time) and $\langle \tau_{ww} \rangle^0$, of aqueous Laponite suspensions in the presence of different concentrations of additives. (f) Superposition of normalized mean slow relaxation times $\langle \tau_{ww} \rangle / \langle \tau_{ww} \rangle^0$ vs. normalized waiting time t_w / t_α^∞ for aqueous Laponite suspensions without and with different concentrations of additives. Inset shows conductivity of 12.2 mM aqueous Laponite suspensions in the presence of 1 mM NaCl and KCl as a function of waiting time t_w .

accelerate the aging dynamics of their suspensions when KCl is added to the suspension medium. Conductivity of Laponite suspensions with equal concentrations of NaCl and KCl, measured using a Eutech PC 2700 4-probe setup, are seen to be comparable and greater than the conductivity of Laponite suspensions without any additives (inset of Figure 2f). This indicates that K^+ behaves like Na^+ in aqueous Laponite suspensions. The solid lines in Figures 2a-d are fits to the following equation 25, 26, 40:

$$\langle \tau_{ww} \rangle = \langle \tau_{ww} \rangle^0 \exp\left[\frac{D t_w}{t_\alpha^\infty - t_w}\right] \quad (2)$$

where D is the fragility parameter and $\langle \tau_{ww} \rangle^0$ is the mean α -relaxation time when $t_w \rightarrow 0$. The parameter t_α^∞ is identified as the Vogel time or waiting time at which the dynamics of the sample freezes [25]. The time-scales t_α^∞ and $\langle \tau_{ww} \rangle^0$ for aqueous Laponite suspensions with and without

additives are extracted by fitting the data to eq 2 and are plotted in Figure 2e. In Figure 2f, we superpose the $\langle \tau_{ww} \rangle$ data for all the suspensions (Figures 2a-d) on a universal curve by dividing the horizontal and vertical axes by t_α^∞ and $\langle \tau_{ww} \rangle^0$ respectively. The self-similar curvatures of the data indicate a common underlying mechanism in the aging of Laponite suspensions with and without additives. The observed increase in $\langle \tau_{ww} \rangle^0$ (shown in dark navy symbols in Figure 2e) and the simultaneous decrease in t_α^∞ (shown in dark purple symbols in Figure 2e) in the presence of the kosmotropes, NaCl and glucose, and the chaotrope KCl point to the increased confinement of Laponite particles in deep potential energy wells and a rapid acceleration in the aging dynamics. However, a decrease in the $\langle \tau_{ww} \rangle^0$ and an increase in t_α^∞ in the presence of DMF indicates shallower potential wells and retarded aging dynamics.

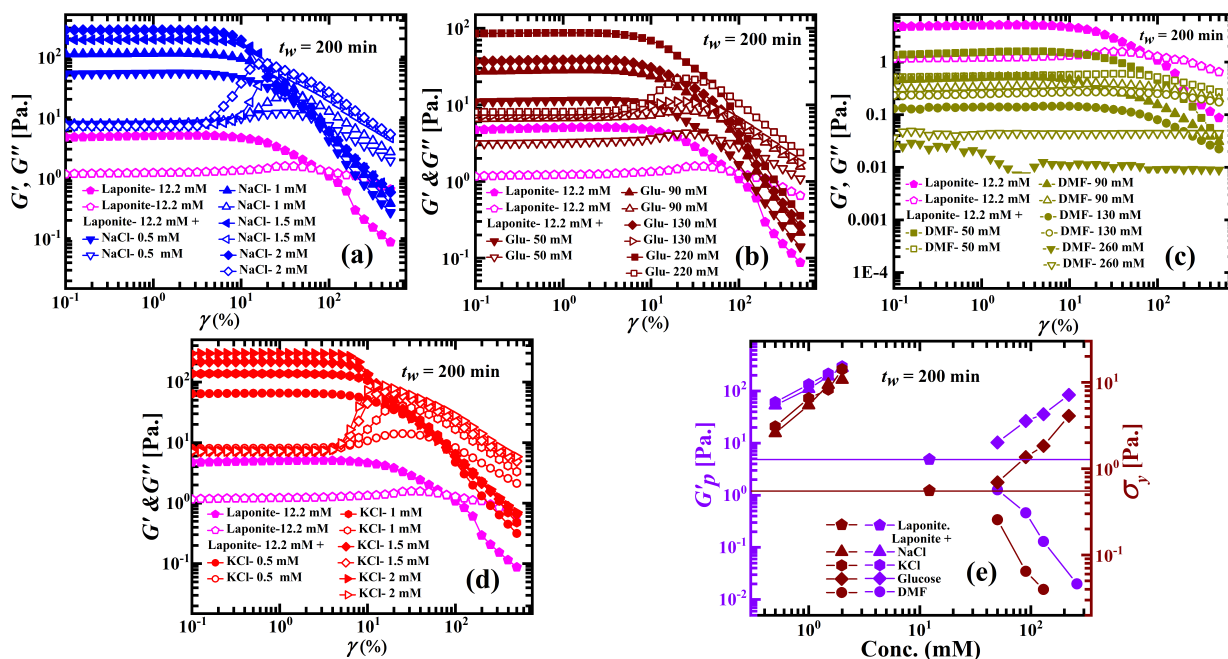


Figure 3: Storage modulus G' (solid symbols) and loss modulus G'' (open symbols) vs. applied oscillatory strain amplitude γ for 12.2 mM aqueous Laponite suspensions in the presence of different concentrations of additives (a) NaCl, (b) glucose (Glu), (c) DMF and (d) KCl at a waiting time $t_w = 200$ min. (e) Plateau values of storage modulus and yield stresses, G'_p and σ_y , of Laponite suspensions without and with additives at $t_w = 200$ min.

We next perform oscillatory strain amplitude sweep experiments to study the viscoelastic properties of aqueous Laponite suspensions with and without additives. The viscoelastic moduli (G' and G'') of 12.2 mM aqueous Laponite suspensions ($t_w = 200$ min) with different concentrations

of additives are plotted as a function of applied strain amplitude in Figures 3a-d. At small values of the strain (in the linear viscoelastic (LVE) regime) the elastic modulus, G' , and the viscous modulus, G'' , are independent of the applied strain, with the elastic modulus dominating over the viscous modulus for the samples with NaCl, glucose, KCl, 50 mM and 90 mM DMF. The suspensions start yielding with an increase in the applied strain amplitude. The onset of this non-linear regime is characterized by a monotonic decrease in G' . Simultaneously, G'' shows a peak at the crossover of G' and G'' before decreasing monotonically. These are typical features of soft glassy systems. At very high strain amplitudes, the suspensions show fluid-like behavior indicated by $G'' > G'$. However, for the Laponite suspensions with the very high DMF concentrations (130 mM and 260 mM DMF in Figure 3e), the viscous modulus is always higher than the elastic modulus, indicating liquid-like behavior in the entire strain window.

It is observed from Figure 3 that at identical waiting times ($t_w = 200$ min), the elasticity (G') of aqueous Laponite suspensions increases with increasing concentration of NaCl and glucose (Figures 3a and b). The addition of DMF, in contrast, reduces the elasticity of the samples (Figure 3c). Figure 3d reveals that the elasticity of the sample increases with increase in KCl concentration. This observation is reasonable considering the acceleration of the physical aging process in the presence of KCl reported earlier using DLS (Figure 2d). In Figure 3e, we plot the plateau values of storage modulus, G'_p (the magnitudes of G' extracted at very low applied strain amplitude γ are shown in violet symbols), and yield stresses, σ_y (shown in wine symbols), of aqueous Laponite suspensions with and without additives at $t_w = 200$ min. The yield stress is calculated from amplitude sweep data following the method proposed by Laurati *et al.* [55]. The details of the analysis and a representative plot are presented in section 1(b) and Figure S3 of the SI. Both G'_p and σ_y , which estimate the strength of the underlying sample microstructures [56], are observed to increase with increasing concentrations of NaCl, glucose and KCl, while they decrease with increasing DMF concentration at $t_w = 200$ min. The increase in G'_p and σ_y for Laponite suspensions in the presence of NaCl, glucose and KCl and their decrease in the presence of DMF arise due to the altered aging dynamics of the samples in the presence of these additives and agree with the DLS results reported earlier.

Figures 4a-d show the evolution of the storage and loss moduli (G' and G'') with waiting time t_w for aqueous Laponite suspensions without and with additives. Soon after preparation, G'' dominates over G' for all the suspensions, thereby indicating viscoelastic liquid-like behavior. As time progresses, both moduli increase, with G' exceeding G'' at a transition time, t_r . The transition

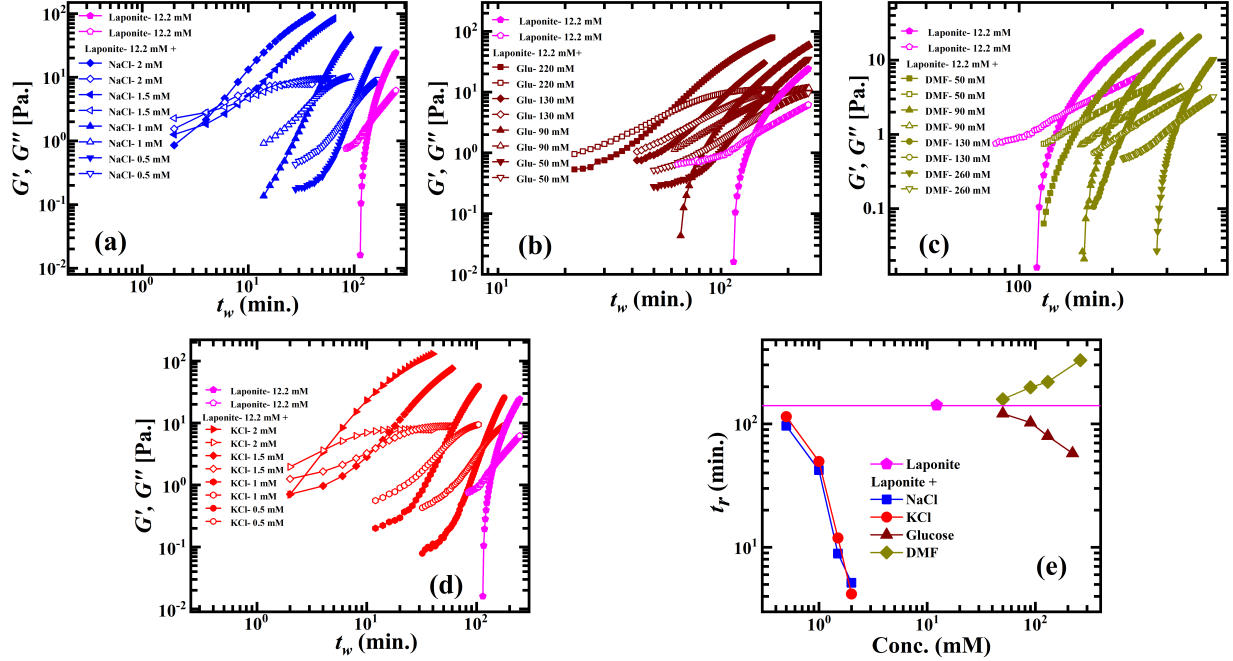


Figure 4: Storage modulus G' (solid symbols) and loss modulus G'' (open symbols) vs. t_w for 12.2 mM aqueous Laponite suspensions in the presence of different concentrations of additives (a) NaCl, (b) glucose (Glu), (c) DMF and (d) KCl. (e) The transition time t_r at which a viscoelastic liquid transforms to a viscoelastic solid (time at which $G' = G''$) for Laponite suspensions with and without additives.

times, t_r , at which the viscoelastic liquid transforms to a viscoelastic solid are plotted in Figure 4e. It is observed from this figure that the transition of aqueous Laponite suspensions from viscoelastic liquid to viscoelastic solid occurs earlier when the kosmotropes, NaCl and glucose, and the chaotrope KCl are added to the suspension. In contrast, the transition is retarded when the chaotrope DMF is added. We attempt to superpose the storage and loss moduli measured in oscillatory strain sweep and time test rheological experiments in Figure S4. It is observed that while the microscopic dynamics and rheological responses in the limit of low strains collapse well, the long-term aging behavior and the mechanical response of Laponite suspensions at high strains are sensitive to the presence of additives.

Finally, we perform cryo-SEM experiments to investigate the morphologies of the samples studied here. Figures 5a-e display the gel-like microstructures of aqueous Laponite suspensions with and without additives at a waiting time of 24 h. Honeycomb like network structures are seen in all samples, with pore sizes that are sensitive to the additive present in the suspension. We note the existence of holes on the flat surfaces of the network branches, indicating the possibility of

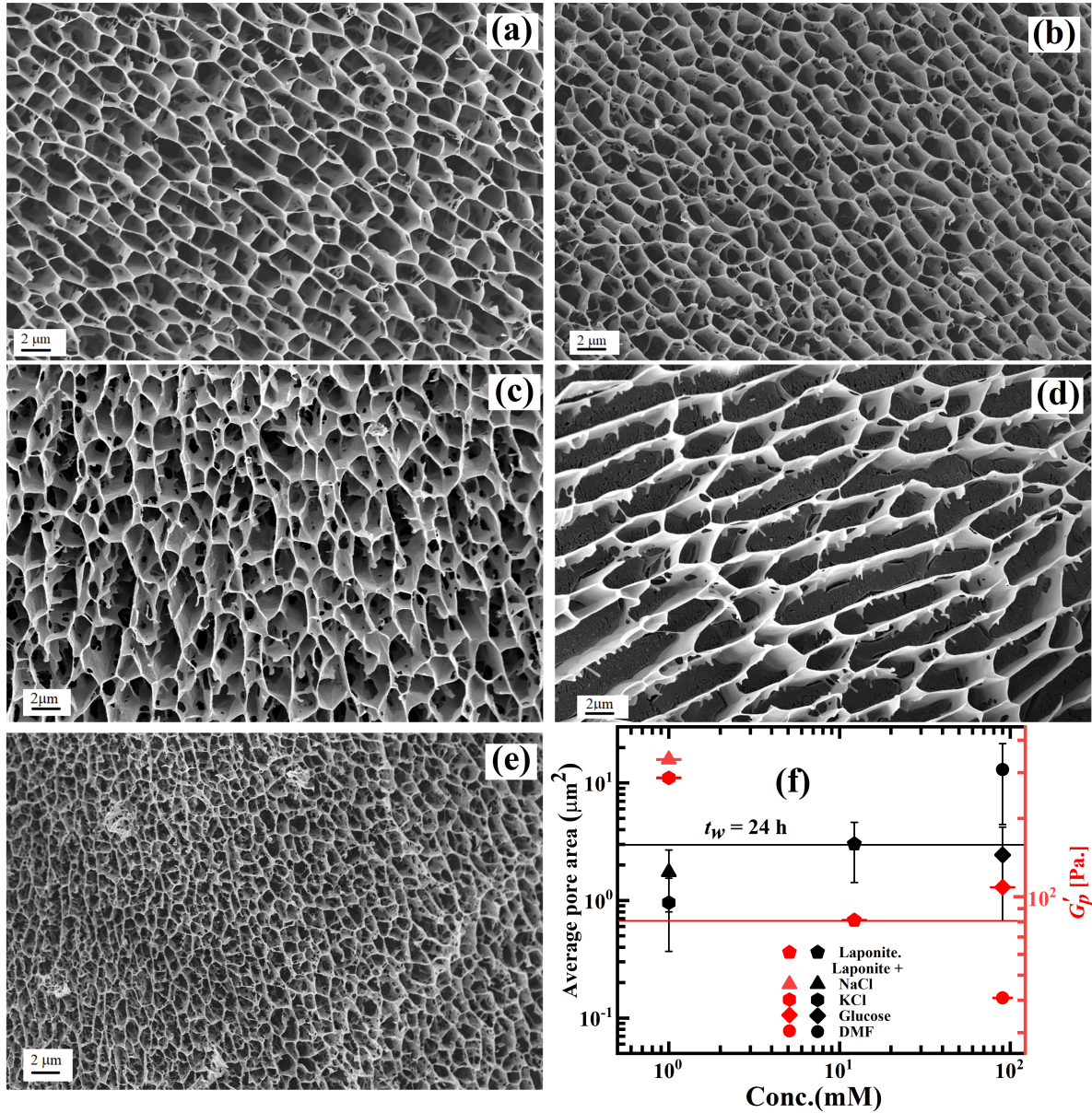


Figure 5: Representative cryo-SEM micrograph for (a) 12.2 mM aqueous Laponite suspension and Laponite suspensions in the presence of (b) 1 mM NaCl, (c) 90 mM glucose, (d) 90 mM DMF and (e) 1 mM KCl at $t_w = 24$ h. (f) Average pore area (black) and plateau values of storage modulus (red) for aqueous Laponite suspensions without and with additives at $t_w = 24$ h.

overlapping coin configurations (OC) of the Laponite platelets [56, 57]. Monte Carlo simulations of suspensions of charged disklike particles at various volume fractions and with different salt concentrations [30, 58] have reported that an OC configuration arises when the positive edge of a platelet parallelly attaches to the edge of the negatively charged face of another platelet, leading to

the formation of long sheets. The magnified cryo-SEM micrographs of all these gels are provided in Figure S5.

We adopt a protocol used earlier [56] to quantify the gel structures by estimating pore areas (data at $t_w = 24$ h is shown in black symbols in Figure 5f) and branch thicknesses (Figure S6). In the analysis of cryo-SEM images, the presence of vitrified water on the structures can lead to the overestimation of the network branch thickness and the simultaneous underestimation of average pore area. However, since the sublimation time (15 min) after cutting the vitrified samples is identical in all the experiments, an equal sublimation-depth is expected for all the samples studied using cryo-SEM. We next correlate the network morphologies with their mechanical responses obtained in rheological experiments. The plateau values of the storage moduli, G'_p (magnitude of G' of these gels at $t_w = 24$ h extracted at very low applied strain amplitude γ (Figure S7)), are also plotted in Figure 5f (shown in red symbols). While the branch thicknesses of the gels remain unchanged in all the samples studied here, it is noted that at a fixed waiting time, the average pore area decreases for Laponite suspensions in the presence of NaCl (\blacktriangle), glucose (\blacklozenge) and KCl (\blacklozenge). Figure 5f displays a simultaneous increase in the elasticity of these samples. On the other hand, an increase in the average pore area and a simultaneous decrease in elasticity is noted when DMF (\bullet) is added to Laponite suspensions (Figure 5f). Many small dangling branches are observed in the walls of the gel network in Figure 5d indicating incomplete structure formation and retarded aging dynamics due to the addition of 90 mM DMF to aqueous Laponite suspensions. In Figure S8, we show the microstructures of aqueous Laponite suspensions in the presence of all the additives at $t_w = 200$ min. When NaCl, glucose and KCl are added to Laponite suspensions, gel-like structures with pore areas larger than those observed in the same samples at a longer waiting time ($t_w = 24$ h) are seen (Figure S8f). Incomplete structure formation is clearly seen in the aqueous Laponite suspension without any additives (Figures S8a) and in the suspension with DMF (Figures S8d). Clearly, aqueous Laponite suspensions age faster in the presence of the kosmotropes, NaCl and glucose, and the chaotrope KCl, while their aging dynamics are retarded in the presence of the chaotrope DMF.

Effect of temperature

Figure 6a plots the dependence of the mean slow α - relaxation time, $\langle\tau_{ww}\rangle$, estimated from DLS experiments, on t_w for aqueous Laponite suspensions at different temperatures. Since an

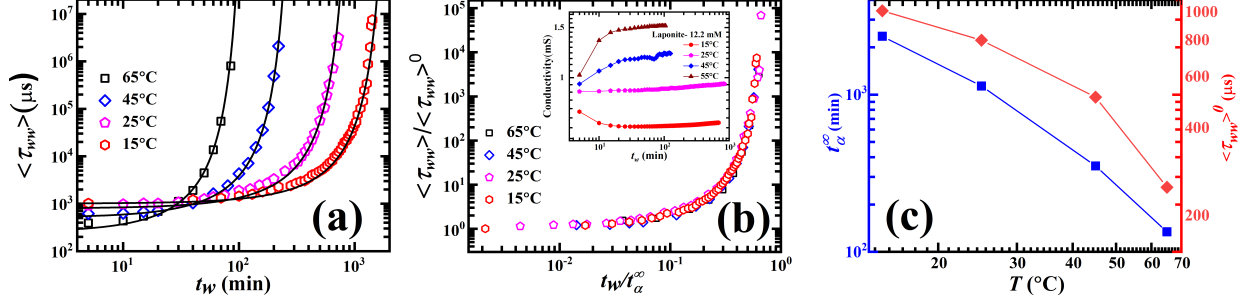


Figure 6: (a) Mean slow relaxation time $\langle \tau_{ww} \rangle$ vs. waiting time t_w for 12.2 mM aqueous Laponite suspensions at different temperatures. The solid lines are fits to eq 2. (b) Superposition of normalized mean slow relaxation times $\langle \tau_{ww} \rangle / \langle \tau_{ww} \rangle^0$ vs. normalized waiting times t_w / t_α^∞ . Inset shows the conductivity of the aqueous Laponite suspensions at different temperatures as a function of t_w . (c) Horizontal and vertical shift factors, t_α^∞ (Vogel time) and $\langle \tau_{ww} \rangle^0$, of aqueous Laponite suspensions at different temperatures.

increase in temperature ruptures the hydrogen bonds in liquid water, increasing the suspension temperature is expected to result in delayed aging dynamics. Surprisingly, the reverse trend is observed for the suspensions studied here, with higher suspension temperatures resulting in accelerated aging dynamics. This unexpected behavior has been reported in an earlier work [26] and can be explained by considering the competition between the chaotropic action of temperature and the kosmotropic action of Na^+ ions that diffuse out of the spaces between Laponite particles. The diffusion of Na^+ ions from the basal planes of Laponite particles is enhanced when temperature is increased (conductivity plotted in the inset of Figure 6b). This effect dominates over the chaotropic action of temperature and results in enhanced inter-particle screening due to the increased participation of Na^+ in EDL formation. The aging dynamics of aqueous Laponite suspensions are therefore accelerated when the temperature is raised. The superposition plot of the $\langle \tau_{ww} \rangle$ data (Figure 6b), obtained by shifting the horizontal and vertical axes, shows self-similar behavior, thereby revealing an indistinguishable aging mechanism of aqueous Laponite suspensions at all temperatures [26]. The horizontal and vertical shift factors, t_α^∞ and $\langle \tau_{ww} \rangle^0$ (extracted by fitting the data in Figure 6a to eq 2) respectively, are plotted in Figure 6c. The observed decreases in $\langle \tau_{ww} \rangle^0$ (displayed in Figure 6c using red symbols) reveals the initial chaotropic effect of the temperature. On the other hand, a decrease in t_α^∞ (displayed in Figure 6c using blue symbols) with increasing temperature indicates an increase in the rate of structure buildup and the acceleration of aging dynamics in the samples.

Next, oscillatory amplitude sweep experiments are performed to study the viscoelastic behav-

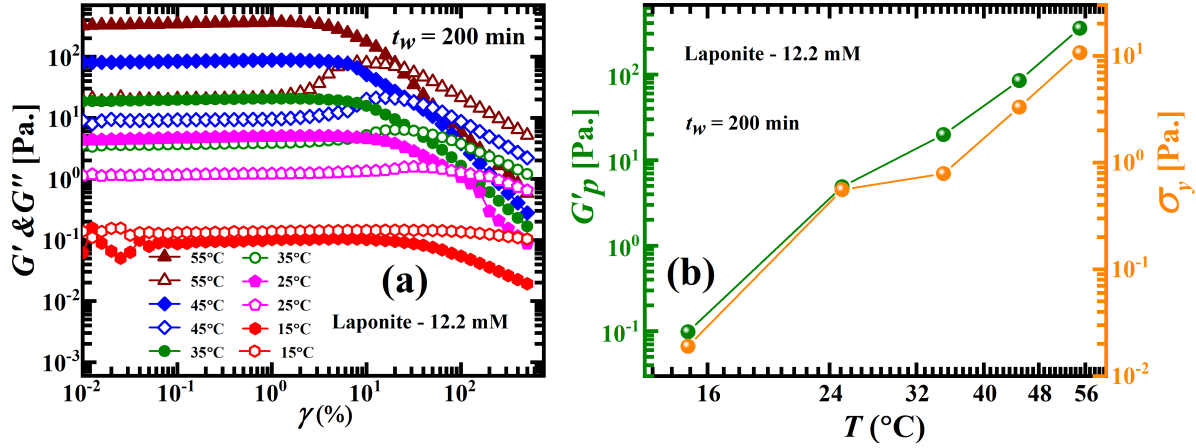


Figure 7: (a) Storage modulus G' (solid symbol) and loss modulus G'' (open symbol) vs. applied oscillatory strain amplitude γ for 12.2 mM aqueous Laponite suspension at different temperatures at $t_w = 200$ min. (b) Plateau values of storage modulus and yield stresses, G'_p and σ_y , of Laponite at $t_w = 200$ min for temperatures in the range 15-55°C.

ior of aqueous Laponite suspensions at different suspension temperatures. Figure 7a shows the temperature dependence of the viscoelastic moduli (G' and G'') of 12.2 mM aqueous Laponite suspensions at $t_w = 200$ min as a function of applied strain amplitude, γ . It is noted that the plateau values of the elastic modulus, G'_p (olive symbols), and yield stresses, σ_y (orange symbols), of aqueous Laponite suspensions increase with temperature (Figure 7(b)). This observed increases in G'_p and σ_y reveal enhancement in the rate of structure buildup [56] and hence accelerated aging dynamics of the samples with increasing suspension temperature and are in agreement with the results of the DLS experiments reported in Figure 6.

The evolution of the viscoelastic moduli (G' and G'') with waiting time, t_w , at different temperatures is shown in Figure 8a. Soon after sample preparation, G'' dominates over G' , showing viscoelastic liquid-like behavior. Both moduli increase with t_w and a transition from a viscoelastic liquid to a viscoelastic solid ($G' = G''$) is noted at a time t_r . The observed decrease in t_r with increasing suspension temperature (Figure 8b) indicates a suppression of the chaotropic action of temperature by the kosmotropic action of the Na^+ ions that form the EDL. This results in the observed acceleration of the aging dynamics and the rapid approach to kinetic arrest when suspension temperature is raised. In Figure S9, we attempt to superpose the storage and loss moduli measured in oscillatory amplitude sweep and time test rheological experiments. Similar to the observations in Laponite suspensions with additives, we note that while the microscopic dynam-

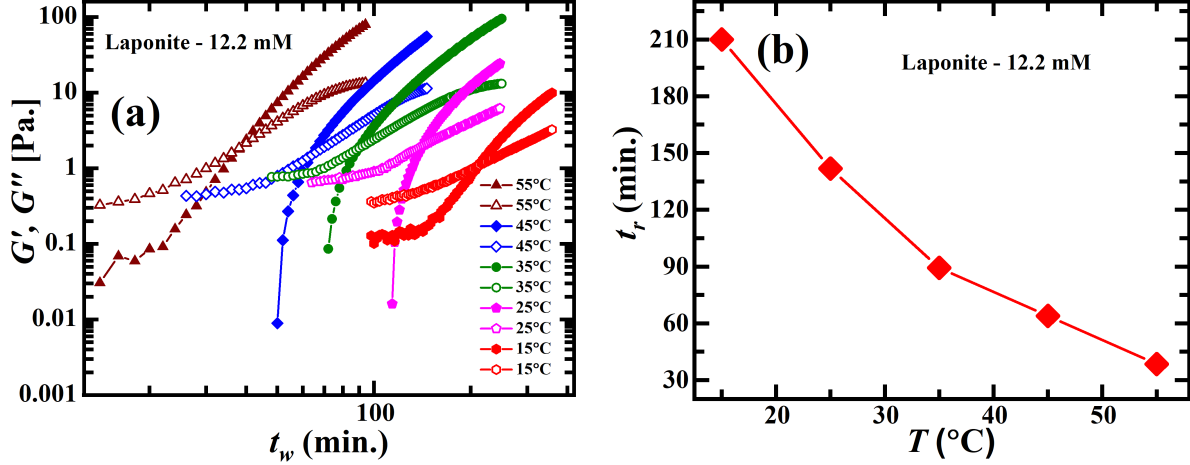


Figure 8: (a) Storage modulus G' (solid symbol) and loss modulus G'' (open symbol) vs. waiting time, t_w , for 12.2 mM aqueous Laponite suspension at different suspension temperatures. (b) Transition times t_r (for transformation of the viscoelastic liquid to a viscoelastic solid, designated by $G' = G''$) at different temperatures.

ics and linear rheological responses collapse well at all temperatures, the bulk dynamics do not superpose over the entire experimental time and strain windows. Clearly, the long-term aging and nonlinear rheology of the samples are sensitive to changes in suspension temperature.

SUMMARY AND CONCLUSIONS

In this study, we have shown that the structure and temperature of the medium significantly affect the aging dynamics of aqueous suspensions of the colloidal clay Laponite. An acceleration in the aging dynamics of the Laponite suspensions was observed when the population of hydrogen bonds in water was increased by adding the kosmotropic molecules NaCl and glucose [45–48]. The enhancement in the local population of hydrogen bonds, induced by the addition of these molecules, results in large osmotic pressure gradients that are directly responsible for the accelerated aging dynamics of the Laponite suspensions studied here. On the contrary, the aging mechanism, facilitated by the sodium counterions present in the intra-tactoidal spaces, was suppressed when the hydrogen bonds in the suspension medium were disrupted by adding DMF [45, 50, 51]. Surprisingly, an acceleration in the aging dynamics was observed when KCl, known to exhibit chaotropic activity in water [46], was added. This result was explained by considering the participation of K^+ in the electric double layer formed by Na^+ that are dissociated from

the faces of the Laponite platelets in aqueous suspension. Rheological experiments, performed to study the effects of the structure of the suspension medium on the aging dynamics of aqueous Laponite suspensions, verify the results of our DLS experiments. Direct imaging using cryogenic scanning electron microscopy (cryo-SEM) reveal that aging Laponite suspensions, in the presence of different additives, form honeycomb like network structures through attractive overlapping coin (OC) configurations. Changes in pore area, estimated from cryo-SEM micrographs, can be correlated to changes in the gel elasticity and the speed of the aging dynamics of the suspensions.

The effect of temperature on the aging dynamics of aqueous Laponite suspensions was also studied. Even though an increase in the temperature of the suspension medium is expected to have a chaotropic effect, the increased dissociation of sodium counterions, confirmed by conductivity measurements, leads to accelerated aging when medium temperature is raised. The strength and population of hydrogen bonds can be altered both by incorporating additives or by changing the suspension temperature. Interestingly, the changes in the microscopic dynamics and rheological properties of aqueous Laponite suspensions were found to be comparable in both situations.

Our results are sufficiently general and can be extended to suspensions of other charged clays such as sodium bentonite and kaolinite. The results reported here will be useful in many applications involving the non-equilibrium dynamics of materials, such as in cosmetics, pharmaceutical products, food industries etc. and in understanding large scale geophysical phenomena such as landslides, earthquakes and the formation of wet quicksands and river deltas.

ACKNOWLEDGEMENTS

We thank Ananya Saha for her help during the initial stages of the experiments and K. M. Yatheendran for his help with cryo-SEM imaging. We thank Raman Research Institute for funding our research and DST SERB (grant number EMR/2016/006757) for partial financial support.

REFERENCES

* Electronic address: ranjini@rri.res.in

- [1] B. Ruzicka, E. Zaccarelli. A fresh look at the Laponite phase diagram. *Soft Matter* **2011**, 7, 1268-1286.

- [2] A. Mourchid *et al.* Phase Diagram of Colloidal Dispersions of Anisotropic Charged Particles: Equilibrium Properties, Structure, and Rheology of Laponite Suspensions. *Langmuir* **1995**, 11, 6, 1942-1950.
- [3] S. Jabbari-Farouji, H. Tanaka, G. Wegdam, D. Bonn. Multiple nonergodic disordered states in Laponite suspensions: A phase diagram. *Physical Review E* **2008**, 78, 061405.
- [4] S. Jatav, Y. M. Joshi. Phase Behavior of Aqueous Suspension of Laponite: New Insights with Microscopic Evidence. *Langmuir* **2017**, 33, 9, 2370-2377.
- [5] A. E. Howayek *et al.* Microstructure of Sand-Laponite-Water Systems using Cryo-SEM. *Geo-Congress Technical Papers* **2014**.
- [6] D. Saha, Y. M. Joshi, R. Bandyopadhyay. Kinetics of the glass transition of fragile soft colloidal suspensions. *The Journal of Chemical Physics* **2015**, 143, 214901.
- [7] R. Bandyopadhyay *et al.* Evolution of Particle-Scale Dynamics in an Aging Clay Suspension. *Physical Review Letters* **2004**, 93, 228302.
- [8] K. Suman, Y. M. Joshi. Microstructure and Soft Glassy Dynamics of an Aqueous Laponite Dispersion. *Langmuir* **2018**, 34, 44, 13079-13103.
- [9] A. Mourchid, E. Lecolier, H. Van Damme, P. Levitz. On Viscoelastic, Birefringent, and Swelling Properties of Laponite Clay Suspensions: Revisited Phase Diagram. *Langmuir* **1998**, 14, 17, 4718-4723.
- [10] R. Bandyopadhyay, P. H. Mohan, Y. M. Joshi. Stress relaxation in aging soft colloidal glasses. *Soft Matter* **2010**, 6, 1462-1466.
- [11] K. Suman, Y. M. Joshi. Analyzing onset of nonlinearity of a colloidal gel at the critical point. *Journal of Rheology* **2019**, 63, 991.
- [12] G. Mallikarjunachari, T. Nallamilli, P. Ravindran, Madivala G. Basavaraj. Nanoindentation of clay colloidosomes. *Colloids and Surfaces A: Physicochemical and Engineering Aspects* **2018**, 550, 167-175.
- [13] F. Bergaya, G. Lagaly. *Handbook of Clay Science*. Elsevier **2013**, 5, 1-19.
- [14] B. Additives, L.P. A. Instruments, Technical brochures on <http://www.byk.com/>, 23.12. **2014**.
- [15] F. Uddin. Clays, Nanoclays, and Montmorillonite Minerals. *Metall. Mater. Trans. A* **2008**, 39, 2804-2814
- [16] W. N. Martens, R. L. Frost, J. Kristof, E. Horvath. Modification of kaolinite surfaces through intercalation with deuterated dimethylsulfoxide. *The Journal of Chemical Physics B* **2002**, 106, 4162-4171.
- [17] E. Mako, J. Kristof, E. Horvath, V. Vagvolgyi. Kaolinite- $\text{Å}\text{S}\text{urea}$ complexes obtained by

- mechanochemical and aqueous suspension techniques-a comparative study, *Journal of Colloid and Interface Science* **2009**, 330, 367-373.
- [18] H. H. Murray. Traditional and new applications for kaolin, smectite, and palygorskite: a general overview. *Appl. Clay Sci.* **2000**, 17, 207-221.
- [19] C. Viseras, C. Aguzzi, P. Cerezo, A. Lopez-Galindo. Uses of clay minerals in semisolid health care and therapeutic products. *Appl. Clay Sci.* **2007**, 36, 37-50.
- [20] A. Thill *et al.* Evolution of particle size and concentration in the RhÃt'ne river mixing zone:: influence of salt flocculation. *Continental Shelf Research* **2001**, 21, 18, 2127-2140.
- [21] A. Khaldoun, E. Eiser, G. Wegdam, D. Bonn. Liquefaction of quicksand under stress. *Nature* **2005**, 437, 7059, 635.
- [22] M. Santagata *et al.* Rheology of concentrated bentonite dispersions treated with sodium pyrophosphate for application in mitigating earthquake-induced liquefaction. *Applied Clay Science* **2014**, 99, 24-34.
- [23] J. Madejova, J. Bujdak, M. Janek, P. Komadel. Comparative FT-IR study of structural modifications during acid treatment of dioctahedral smectites and hectorite. *Spectrochimica Acta Part A* **1998**, 54, 1397-1406.
- [24] B. Ruzicka, L. Zulian, G. Ruocco. Routes to Gelation in a Clay Suspension. *Physical Review Letters* **2004**, 93, 25, 258301.
- [25] D. Saha, Y. M. Joshi, R. Bandyopadhyay. Investigation of the dynamical slowing down process in soft glassy colloidal suspensions: comparisons with supercooled liquids. *Soft Matter* **2014**, 10, 3292-3300.
- [26] D. Saha, R. Bandyopadhyay, Y. M. Joshi. Dynamic Light Scattering Study and DLVO Analysis of Physicochemical Interactions in Colloidal Suspensions of Charged Disks. *Langmuir* **2015**, 31, 10, 3012-3020.
- [27] Y. M. Joshi. Model for cage formation in colloidal suspension of laponite. *The Journal of Chemical Physics* **2007**, 127, 8, 081102.
- [28] S. Ali, R. Bandyopadhyay. Use of Ultrasound Attenuation Spectroscopy to Determine the Size Distribution of Clay Tactoids in Aqueous Suspensions. *Langmuir* **2013**, 29, 41 12663-12669.
- [29] S. L. Tawari, D. L. Koch, C. Cohen. Electrical Double-Layer Effects on the Brownian Diffusivity and Aggregation Rate of Laponite Clay Particles. *Journal of Colloid and Interface Science* **2001**, 240 1 54-66.
- [30] M. Delhorme, B. Jonsson, C. Labbez. Monte Carlo simulations of a clay inspired model suspension: the role of rim charge. *Soft Matter* **2012**, 8, 9691-9704.

- [31] M. Delhomme, B. Jonsson, C. Labbez. Gel, glass and nematic states of plate-like particle suspensions: charge anisotropy and size effects. *RSC Adv.* **2014**, 4, 34793-34800.
- [32] B. Abou, D. Bonn, and J. Meunier. Aging dynamics in a colloidal glass. *Physical Review E* **2001**, 64, 021510.
- [33] D. Bonn *et al.* Aging of a colloidal "Wigner" glass. *Europhys Lett* **1999**, 45, 1, 52.
- [34] T. Nicolai, S. Cocard. Dynamic Light-Scattering Study of Aggregating and Gelling Colloidal Disks. *Journal of Colloid and Interface Science* **2001**, 244, 1, 51-57.
- [35] P. Mongondry, J. F. Tassin, T. Nicolai. Revised state diagram of Laponite dispersions. *Journal of Colloid and Interface Science* **2005**, 283, 2, 397-405.
- [36] V. T. Ranganathan, R. Bandyopadhyay. Effects of aging on the yielding behaviour of acid and salt induced Laponite gels. *Colloids and Surfaces A: Physicochemical and Engineering Aspects* **2017**, 522, 304-309.
- [37] P. Gadige, R. Bandyopadhyay. Electric field induced gelation in aqueous nanoclay suspensions. *Soft Matter* **2018**, 14, 6974-6982.
- [38] S. Jatav, Y. M. Joshi. Chemical stability of Laponite in aqueous media. *Applied Clay Science* **2014**, 97-98, 72-77.
- [39] D. W. Thompson, J. T. Butterworth. The nature of laponite and its aqueous dispersions. *Journal of Colloid and Interface Science* **1992**, 151, 1, 236-243.
- [40] P. Gadige, D. Saha, S. K. Behera, R. Bandyopadhyay. Study of dynamical heterogeneities in colloidal nanoclay suspensions approaching dynamical arrest. *Scientific Reports* **2017**, 7, 8017.
- [41] B. Hribar, N. T. Southall, V. Vlachy, K. A. Dill. How Ions Affect the Structure of Water. *Journal of the American Chemical Society* **2002**, 124, 41, 12302-12311.
- [42] A. Mudi, C. Chakravarty. Effect of Ionic Solutes on the Hydrogen Bond Network Dynamics of Water: Power Spectral Analysis of Aqueous NaCl Solutions. *The Journal of Physical Chemistry B* **2006**, 110, 16, 8422-8431.
- [43] J. D. Smith *et al.* Unified description of temperature-dependent hydrogen-bond rearrangements in liquid water. *PNAS* **2005**, 102, 40, 14171-14174.
- [44] R. Ludwig. Water: From Clusters to the Bulk. *Angew. Chem. Int. Ed.* **2001**, 40, 10, 1808-1827.
- [45] P. M. Geethu, V. T. Ranganathan, Dillip K. Satapathy. Inferences on hydrogen bond networks in water from isopermittive frequency investigations. *Journal of Physics: Condensed Matter* **2018**, 30, 315103.
- [46] P. B. Ishai, E. Mamontov, J. D. Nickels, A. P. Sokolov. Influence of ions on water diffusion-a neutron

- scattering study. *The Journal of Physical Chemistry B* **2013**, 117, 25, 7724-7728.
- [47] X. Ma, M. Pawlik. Adsorption of guar gum onto quartz from dilute mixed electrolyte solutions. *Journal of colloid and interface science* **2006**, 298, 2, 609-614.
- [48] M. Paolantoni, P. Sassi, A. Morresi, S. Santini. Hydrogen bond dynamics and water structure in glucose-water solutions by depolarized Rayleigh scattering and low-frequency Raman spectroscopy. *The Journal of Chemical Physics* **2007**, 127, 024504.
- [49] J. W. Brady. Molecular dynamics simulations of .alpha.-D-glucose in aqueous solution. *Journal of the American Chemical Society* **1989**, 111, 14, 5155-5165.
- [50] Y. Lei, H. Li, H. Pan, S. Han. Structures and Hydrogen Bonding Analysis of N,N-Dimethylformamide and N,N-Dimethylformamide-Water Mixtures by Molecular Dynamics Simulations. *the Journal of Physical Chemistry A* **2003**, 107, 10, 1574-1583.
- [51] J. M. M. Cordeiro, L. C. Gomide Freitas. Study of Water and Dimethylformamide Interaction by Computer Simulation. *Zeitschrift fur Naturforschung A* **1999**, 54, 2, 110-116.
- [52] B. J. Berne, R. Pecora, *Dynamic Light Scattering: With Applications to Chemistry. Biology and Physics* (John Wiley & Sons, New York, **1975**).
- [53] C. P. Lindsey, G. D. Patterson. Detailed comparison of the Williams-Watts and Cole-DeDavidson functions. *The Journal of Chemical Physics* **1980**, 73, 3348.
- [54] J. Cannon, D. Kim, S. Maruyama, J. Shiomi. Influence of ion size and charge on osmosis. *The Journal of Physical Chemistry B* **2012**, 116, 14, 4206-4211.
- [55] M. Laurati, S. U. Egelhaaf, G. Petekidis. Nonlinear rheology of colloidal gels with intermediate volume fraction. *J. Rheol* **2011**, 55, 673-706.
- [56] S. Ali, R. Bandyopadhyay. Effect of electrolytes on the microstructure and yielding of aqueous dispersions of colloidal clay. *Soft Matter* **2016**, 12, 414-421.
- [57] S. Ali, R. Bandyopadhyay. Aggregation and stability of anisotropic charged clay colloids in aqueous medium in the presence of salt. *Faraday Discuss* **2016**, 186, 455-471.
- [58] B. Jonsson, C. Labbez, B. Cabane. Interaction of Nanometric Clay Platelets. *Langmuir* **2008**, 24, 20, 11406-11413.

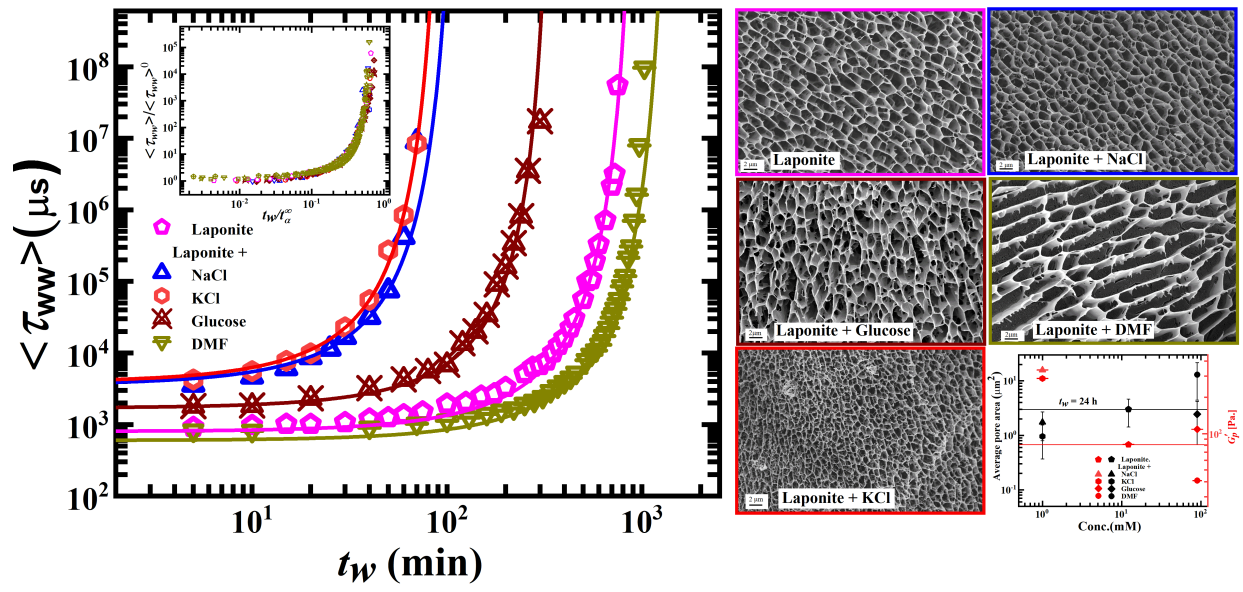


Figure 9: Table of contents only.